

Photoinduced intersubband transition in undoped HgCdTe multiple quantum wells

C. R. M. de Oliveira, A. M. de Paula,^{a)} and C. L. Cesar
Instituto de Física, Universidade Estadual de Campinas, 13083-970 Campinas-SP, Brazil

L. C. West,^{b)} C. Roberts,^{b)} R. D. Feldman, and R. F. Austin
AT&T Bell Laboratories, Holmdel, New Jersey 07733

M. N. Islam
University of Michigan, Ann Arbor, Michigan 48109

G. E. Marques
Departamento de Física, Universidade Federal de São Carlos, 13565-905, São Carlos SP, Brazil

(Received 3 January 1995; accepted for publication 2 April 1995)

We present photoinduced intersubband absorption measurements in HgCdTe undoped quantum wells. The transition energies and the linewidths are well described by a full $8 \times 8 \mathbf{k} \cdot \mathbf{p}$ Kane model calculation. Also, based on this model we show that different in-plane effective masses for the first and second electron subbands should be considered in order to properly fit the low energy side of the experimental spectra. The experimental results can be explained using the calculated intersubband oscillator strength with no exciton enhancement. © 1995 American Institute of Physics.

Intersubband transitions in quantum well structures are of considerable interest because of their potential applications in infrared optical modulators, lasers, detectors and emitters. West and Eglash first observed the optical absorption transition between the first and second electron subbands in GaAs/AlGaAs modulation doped quantum wells,¹ and they measured an oscillator strength which agreed with the quantum mechanical predictions. Similar results were obtained by Levine *et al.*² considering that their definition of the oscillator strength which uses the electron effective mass instead of the free-electron mass. Measurements of intersubband transition absorption via photopumping of the conduction band in undoped GaAs/AlGaAs quantum wells³ have indicated a possible enhancement of the oscillator strength due to excitonic effects, specially at low temperatures, as compared to those of doped quantum wells.² However, the observation of this enhanced oscillator strength depends on an accurate assessment of a number of experimental parameters involved in the estimation of the induced charge in the conduction band.⁴

In this letter we present photoinduced intersubband absorption measurements in HgCdTe multiple quantum wells (MQW). The transition energies and the linewidths are calculated in a full $8 \times 8 \mathbf{k} \cdot \mathbf{p}$ Kane model approximation.⁵ Also, based on this model we show that different in-plane effective masses for the first and second electron subbands should be considered in order to properly fit the low energy side of the experimental spectra. The experimental results can be explained using the calculated intersubband oscillator strength with no exciton enhancement.

We studied two undoped MQW samples grown by molecular beam epitaxy on GaAs substrates which consist of 50 periods of a 80 Å thick Hg_{0.60}Cd_{0.40}Te well or a 100 Å thick

Hg_{0.83}Cd_{0.27}Te well, respectively separated by a 100 Å thick Hg_{0.15}Cd_{0.85}Te barrier. Interband absorption characterization and other samples details were presented elsewhere.^{6,7} The photoinduced intersubband absorption spectra were taken in a Fourier transform spectrometer using the sample geometry showed in Fig. 1(a). The infrared light was focused on a 45° sample polished edge in a 120 (± 60) degree external cone

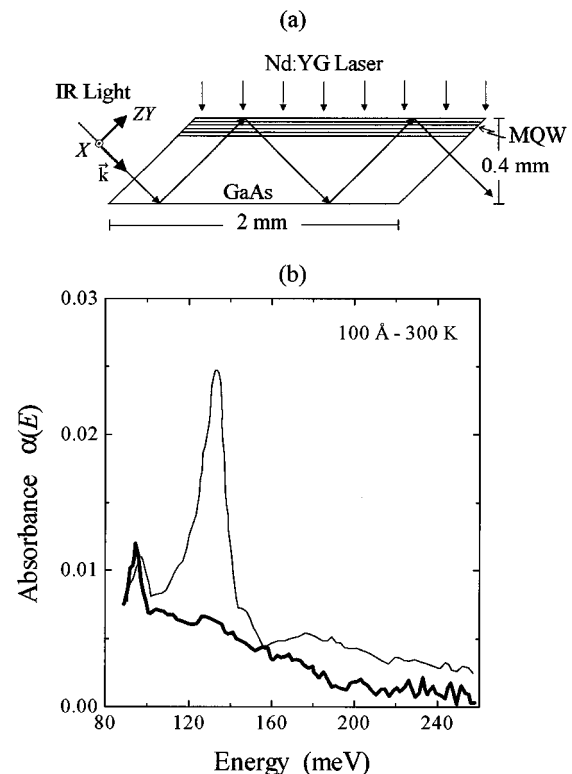


FIG. 1. (a) Details of the infrared (IR) and the pump light path in the sample; (b) Room temperature photoinduced absorption spectra: thick line is the X polarization, thin line is the ZY polarization.

^{a)}Electronic mail: adepaula@ifi.unicamp.br

^{b)}Present address: Integrated Photonic Systems, Inc., 1325 Campus Parkway, Suite 211, Wall Township, NJ 07719.

which will change to a 30 (± 15) degree cone inside the GaAs substrate. It travels in a zigzag pattern, due to total internal reflections, reflecting twice in the sample, i.e., it passes four times through the MQWs. The infrared light polarization can be set parallel to the MQW surface plane (X polarization) and 45° out of the plane (ZY polarization), which is the only one that couples to the intersubband transition. This geometry largely enhances the intersubband absorption compared to the Brewster's angle geometry¹ but it still cannot completely eliminate an in-plane polarization (Y) component. The coupling with the intersubband transition depends on the incidence angle and, in principle, should be averaged from the 45 ± 15 degree cone. Nonetheless we simply assume a straight 45° incidence angle on the MQW. One advantage of this light cone is the averaging out of the Fabry-Pérot fringes, usually seen in transmission spectra. The temperature was controlled with a micro-miniature refrigerator⁸ from MMR Technologies Inc. A 5 W cw Nd:YAG laser coupled to a multimode fiber epoxyed in a hole on the refrigerator wall provided the pump light. This system was able to deliver up to 2 W on a 3 mm spot on the MQW sample surface. The carrier density estimated from the pump details ($P=2$ W, wavelength $\lambda=1.064$ μm , carrier lifetime $\tau=3$ ns and reflection at the sample surface $\approx 25\%$) is $N_0=1 \times 10^{10}$ cm^{-2} .

The photoinduced intersubband absorption spectra were obtained using the unpumped spectrum as the background spectrum, i.e., the absorption intensity is given by $\alpha(E) = \log(\text{unpumped}/\text{pumped-spectra})$. The change in the transmission due to the pump is given by $I_p = I_{\text{unpumped}} \exp(-l\Delta\alpha)$, where l is the optical path length, therefore we get $\alpha(E) = l\Delta\alpha \log e$. The $\alpha(E)$ value will be positive if there is an increase in the absorption due to the pump light. This is the case for the transition from the first to the second electron subband, the pump light populates the first electron subband and enable the absorption in this intersubband transition. Figure 1(b) shows the room temperature intersubband photoinduced spectra for the 100 Å sample at both X and ZY polarization. We can see clearly the positive intersubband transition absorption at the ZY polarization that disappears at the X polarization. Note that at both polarizations the absorption rises toward lower energies which is due to GaAs multiphonon absorption.

Figure 2 shows the intersubband photoinduced spectra at ZY polarization for the two samples studied. In this plot we have used the X polarization spectrum to subtract the phonon contribution from the ZY polarization one. Note that there is a clear tail at the low energy side of the spectra. This tail cannot be explained in a simple effective mass approximation which predicts a single intersubband transition energy. We will show that different in-plane effective masses for the first and the second electron subbands can account for this low energy tail.

We calculate the quantum well band structure using a complete 8×8 $\mathbf{k} \cdot \mathbf{p}$ approximation.⁵ These calculations give interband transition energies that agree with the experimental interband absorption results⁶ within 5 meV. The obtained intersubband transition energies (E_0) are listed in Table I. Figure 3 shows the electron subbands for the two samples stud-

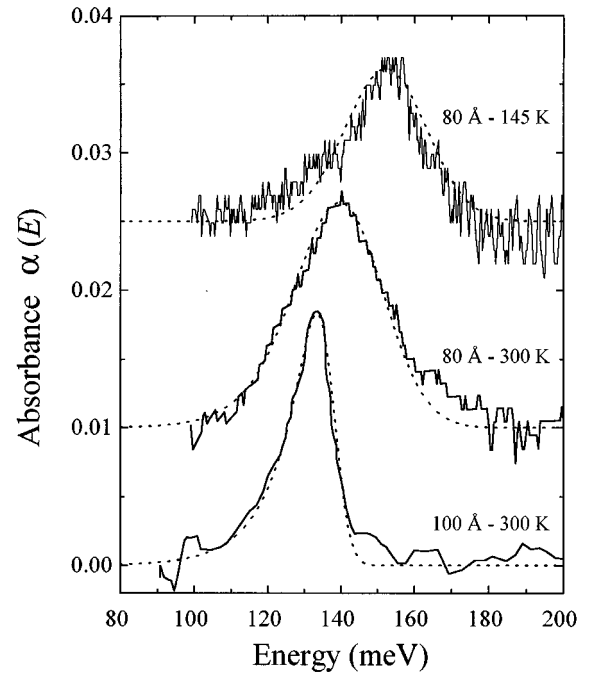


FIG. 2. Photoinduced intersubband absorption spectra for the 80 Å sample at temperatures 145 K and 300 K and for the 100 Å sample at 300 K, solid lines are the experimental spectra and dotted lines are the theoretical fit. The spectra are all at the same scale but they have been displaced vertically for clarity.

ied (solid lines). Note the deviation from a parabolic behavior. Nonetheless we fit a parabola to the calculated low \mathbf{k}_{\parallel} range for the first and second electron subbands (dotted lines) and we obtain an in-plane effective mass for each subband (values are listed in Table I). This is the energy range ($\approx 2kT$) probed by the intersubband absorption spectra. The electron effective mass for the second subband is heavier than for the first subband and, as a consequence, the intersubband transition energy is lower for higher in-plane energy states than at $\mathbf{k}_{\parallel}=0$. This explains the low energy tail observed in the spectra of Fig. 2.

We fit the intersubband spectra with the expression⁹

$$\alpha(E) = \log e \frac{e_e^2 h N_0}{4 \epsilon_0 n m_o c} \frac{\sin^2 \theta}{\cos \theta} W B f_{12} \frac{\mu}{m_{e1} k T} \times \exp\left(\frac{-\mu(E_0 - E)}{m_{e1} k T}\right), \quad (1)$$

where e_e is the electron charge, h is the Planck constant, N_0 is the photoexcited carrier density, ϵ_0 is the vacuum dielectric constant, $n=3$ is the HgCdTe refractive index (aver-

TABLE I. Calculated in-plane effective masses and intersubband transition energies, and the parameters obtained from the fitting of the intersubband absorption spectra.

			E_0 (meV)		N_0 (10^{10} cm^{-2})	Γ (meV)
	m_{e1}	m_{e2}	Cal.	Fit	Fit	Fit
80 Å-145 K	0.056	0.081	148	156	0.9	15
80 Å-300 K	0.056	0.081	140	146	1.5	15
100 Å-300 K	0.039	0.061	132	138	0.6	5

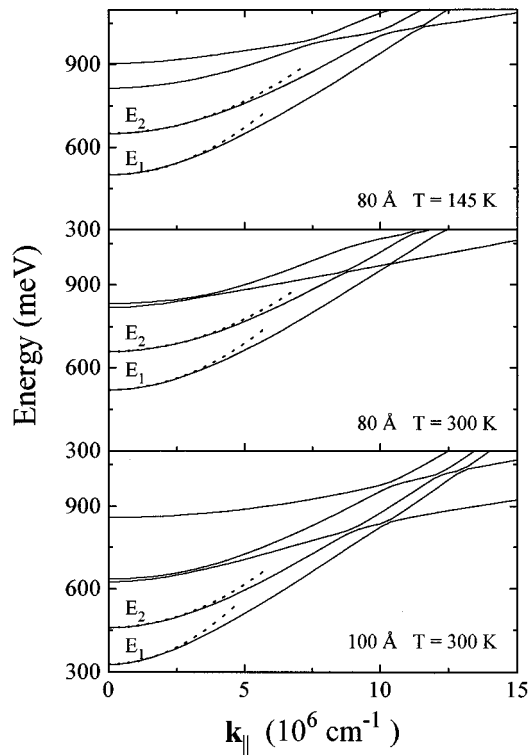


FIG. 3. Calculated electron band structure using the $8 \times 8 \mathbf{k} \cdot \mathbf{p}$ approximation, solid lines. Dotted lines are a parabolic fit to obtain in-plane effective masses for the first and second electron subbands. The energy zero is at the top of the well valence band.

age between well and barrier), m_o is the free-electron mass, c is the light velocity in vacuum, $\theta=45^\circ$ is the incidence angle, $W=50$ is the number of wells, $B=4$ is the number of passes through the wells, f_{12} is the intersubband oscillator strength, k is the Boltzmann constant, and T the sample temperature. The exponential term comes from the Boltzmann distribution factor, with $\mu^{-1} = m_{e1}^{-1} - m_{e2}^{-1}$, where m_{e1} and m_{e2} are the first and second subband in-plane effective masses, respectively, and E_0 is the intersubband transition energy (values in Table I). We consider a phenomenological broadening by performing a convolution of Eq. 1 with a Gaussian of width Γ .

The intersubband oscillator strength¹ is calculated using the electron wave functions obtained considering a finite barrier height V_C and the nonparabolic model of Ref. 6. The V_C values were obtained using the expression for the energy gap of $\text{Hg}_{1-x}\text{Cd}_x\text{Te}$ as a function and the nonparabolic model of Ref. 7. The V_C values were obtained using the expression for the energy gap of $\text{Hg}_{1-x}\text{Cd}_x\text{Te}$ as a function of x and temperature from Ref. 10, and the valence well height $\Delta E_v = (x_b - x_w)VBO$ from Ref. 11, where x_w and x_b are the Cd concentration of the well and barrier layers, respectively, and $VBO=400$ meV is the valence band offset of HgTe-CdTe quantum wells.

The calculated curves in Fig. 2 were obtained with only E_0 , N_0 and Γ as the fitting parameters. The best fitting values are listed in Table I. The values of N_0 needed to fit the experimental results are less than a factor of 2 out of the experimental estimated value. These small differences can be easily explained either by small changes in the pump power

or by changes of the carrier lifetimes at different sample temperatures. We should also point out that the low energy tail in the intersubband spectra is well fitted with the different in-plane effective masses obtained from the $\mathbf{k} \cdot \mathbf{p}$ approximation. The experimental results cannot be reproduced without considering these in-plane effective masses. The Γ values are smaller than the ones needed to fit the interband absorption spectra with this convolution procedure. For instance, for the 100 Å sample we fitted the interband absorption spectra at 300 K and 12 K (see Ref. 6) with $\Gamma = 18$ meV and $\Gamma = 11$ meV, respectively. It is smaller here because the band gap fluctuations, which appear directly in the interband transition, only change the difference in the confined subbands through the effective mass variations. We estimate a $\Delta E_0 = 2$ meV variation when the band gap changes by 11 meV using the nonparabolic model of Ref. 6. Thus the obtained $\Gamma = 5$ meV for the intersubband transition is consistent with the $\Gamma = 18$ meV for the interband absorption. The experimental results can be explained using the calculated intersubband oscillator strength with no exciton, bounded or unbounded, enhancement. HgCdTe multiple quantum wells have not shown clearly resolved excitonic peaks even at low temperature interband absorption, however there is a strong Coulombic enhancement of the absorption due to ionized excitons.⁷ Also the electron-phonon scattering time is expected to be smaller than in GaAs.^{6,12} These two effects may tend to decrease any possible bound exciton contribution.

In conclusion we have measured photoinduced intersubband absorption in HgCdTe undoped quantum wells. We show that different in-plane effective masses for the first and second subbands should be considered in order to properly fit the low energy side of the experimental spectra. The intersubband oscillator strength can be explained using a nonparabolic band model and no excitonic enhancement has been observed.

We acknowledge financial support from CNPq, PADCT, FAPESP, and CPqD.

¹L. C. West and S. J. Eglash, Appl. Phys. Lett. **46**, 1156 (1985).

²B. F. Levine, R. J. Malik, J. Walker, K. K. Choi, C. G. Bethea, D. A. Kleinman, and J. M. Vandenberg, Appl. Phys. Lett. **50**, 273 (1987).

³M. Olszakier, E. Ehrenfreund, E. Cohen, J. Bajaj, and G. J. Sullivan, Phys. Rev. Lett. **62**, 2997 (1989).

⁴E. R. Brown, K. A. McIntosh, and K. B. Nichols, Proc. SPIE **1675**, 260 (1992).

⁵A. M. Cohen and G. E. Marques, Phys. Rev. B **41**, 10608 (1990).

⁶C. L. Cesar, M. N. Islam, R. D. Feldman, R. F. Austin, D. S. Chemla, L. C. West, and A. E. DiGiovanni, Appl. Phys. Lett. **56**, 283 (1990).

⁷R. D. Feldman, R. F. Austin, C. L. Cesar, M. N. Islam, C. E. Socolich, Y. Kim, and A. Ourmazd, Mater. Res. Soc. Symp. Proc. **216**, 113 (1991).

⁸W. A. Little, Physica B & C **109&110**, 2001 (1982).

⁹L. C. West, C. W. Roberts, J. P. Dunkel, T. K. Gaylord, G. N. Henderson, E. Anemogiannis, E. N. Glytsis, and M. T. Asom, Proc. SPIE **2145**, 132, (1994).

¹⁰M. H. Weiler, in *Semiconductors and Semimetals*, edited by R. K. Willardson and A. C. Beer (Academic, London, 1981), Vol. 16, p. 180.

¹¹C. L. Cesar, M. N. Islam, R. D. Feldman, R. Spitzer, R. F. Austin, A. E. DiGiovanni, J. Shah, and J. Orenstein, Appl. Phys. Lett. **54**, 745 (1989).

¹²C. L. Cesar, M. N. Islam, C. E. Socolich, C. E. Socolich, R. D. Feldman, R. F. Austin, and K. R. German, Opt. Lett. **15**, 1147 (1990).